



## **1.1 Brief History of Carbon Family**

A revolution in the scientific society is taking place as researchers are achieving new and significant ways to pattern and characterize materials at the nanometer length. Amongst all, carbon being present in ample amount, has been extensively scrutinized since eighteenth century and accomplished uninterrupted growth forever after. The mushrooming initiated after the synthesis of graphite oxide (termed as ‘Graphon’) by Brodie [1] to identify the molecular weight of graphite. Thereafter, the characteristics of graphite oxide were illustrated by Kohlschütter and Haenni [2] in 1918. Consequently, their structural property was accomplished by Bernal [3] in 1924 via single-crystal diffraction measurements. Eventually when the characterization techniques evolved, Wallace analyzed the electronic properties of graphite and primarily brought the concept of graphene, which laterally recognized as “a wonder material” [4]. Following that, a couple of surfaces of graphite through transmission electron microscopy (TEM) were efficiently observed by Ruess and Vogt [5]. The method to prepare graphite oxide by Brodie [1] was hazardous due to which, Hummers and Offeman [6] designed a harmless, reliable, economical and efficient approach. Later on, Boehm in 1962 [7], elementally conveyed the creation of single layer graphite sheet. In 1984, theoretical physicists DiVincenzo and Mele constructed massless Dirac equation for graphite host and unbelievable at that point in history of nineteenth century [8]. A eureka moment in the scientific world was created when Smally in 1985 [9] invented Buckminsterfullerene ( $C_{60}$ ) and one year later awarded Nobel prize for this miracle discovery. The discovery of fullerene became the first carbon allotrope that stimulated the researchers around the world to explore carbon based materials. The term ‘graphene’ to depict graphite single sheets was given by Mouras et al. in 1987 [10] despite the fact that theoretical calculations were still remained a fiction. A different allotrope of carbon was later on discovered, namely, carbon nanotubes (CNTs) by Iijima in the end of nineteenth century [11]. After more than ten years, a remarkable experiment done by Geim and Novoselov took the moment of entire history of carbon materials [12]. The monolayer graphene was first invented through Scotch tape method and guided the whole research society to investigate two dimensional materials that will lead to more advanced and new technological applications. The efforts on carbon materials again found its way when Geim and Novoselov rewarded a Nobel Prize in 2010 for their worthy

experimental work. The road map of the journey of carbon based materials is presented in Fig. 1.1.

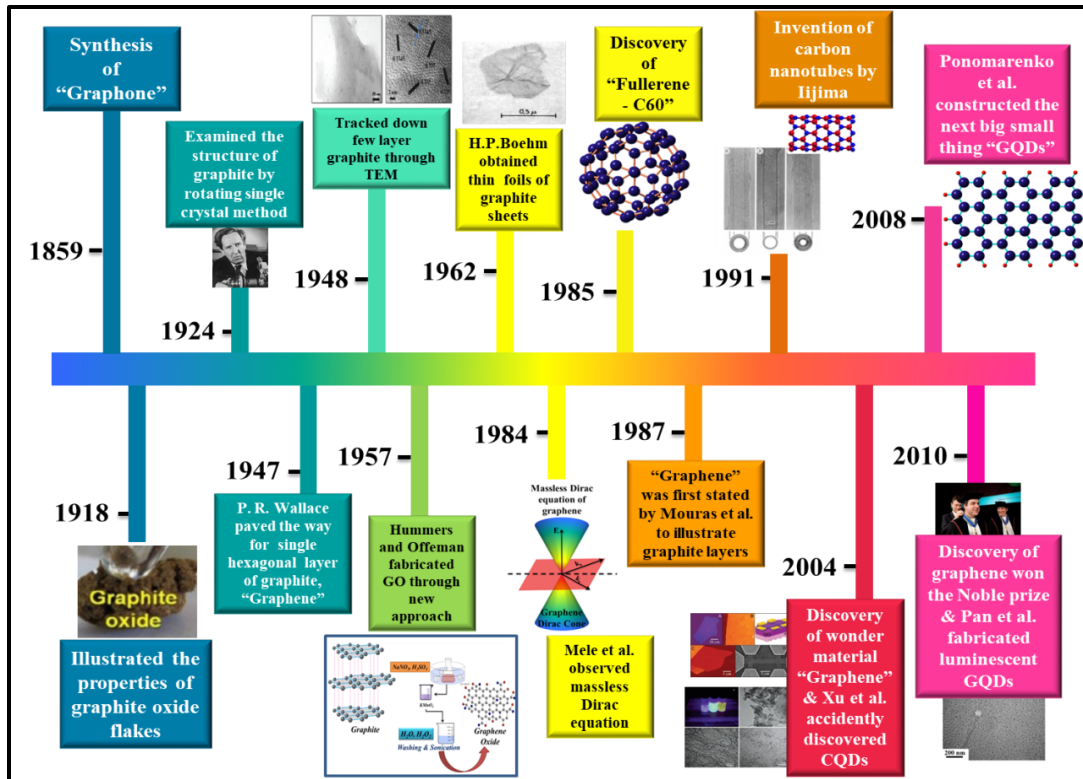


Figure 1.1: Road map of carbon materials - from graphite to graphene quantum dots.

## 1.2 From Graphene to Graphene Quantum Dots

Since the discovery of graphene, it has been an epicenter in the research field due to its extraordinary electronic [13], mechanical [14], optical properties [15] etc. which can be used in numerous applications like OLED, lithium ion batteries, ultra-capacitors, water desalination and many more [16]. Graphene is a semi-metal as the conduction band and valence band overlap slightly forming the Dirac cone. Apart from these fascinating properties of graphene, the notable limitations are zero bandgap, low absorptivity including poor dispersion in solvents and aggregation. Due to the zero bandgap of graphene which is the trait of half-metallic materials, it limits its utilization in the region of optoelectronic devices and semiconductors [17]. In order to overcome the limitations of graphene, various approaches were derived like structural modification, introduction of foreign atoms etc. One significant and promising pathway to

overcome this drawback is to reduce the dimensionality of graphene or simply to cut graphene into nanometer scale pieces. On the basis of work done by Xu et al. on carbon dots (CDs) [18], Ponomarenko and Geim in 2008 came up with ‘Graphene quantum dots (GQDs)’ [19]. These small dots are becoming the next big thing in research society. There are discrepancies between CDs and GQDs such as GQDs size is smaller than 100nm with thickness beneath 10 layers [20] while CDs have size under 10 nm and are generally quasi-spherical [20]. This can be attributed due to the fact that GQDs acquire graphene lattice within the dots. The extraordinary fluorescent properties (strong blue emission) of GQDs were invented by Pan et al. [21] when GQDs are fabricated through hydrothermal route. The reason for this strong fluorescence is the free zigzag site including carbene-like triplet ground state [21]. New materials with noteworthy electrical, magnetic, optical and mechanical properties are promptly evolving for the use in energetic technologies, nanoelectronics, spintronics, environmental applications etc. Over the past few decades group IV-VI quantum dots like CdSe, PbTe, PbSe, CdS, HgTe, ZnSe etc. have attracted a great amount of interest due to their variety of applications comprising optoelectronics, solar cells, light emitting diodes and bio-imaging [22]. These varieties of applications are due to quantum dot’s tunable optical and electrical properties [23]. The major drawback of these colloidal QDs is their intrinsic toxicity and stability which hinders them from many applications. In order to compete with other QDs and different 3D, 2D and 1D materials to be used in many different applications, their capability to adjust and modify for desirable properties is of utmost importance. Alteration in properties of GQDs through doping was primarily studied by Zhao et al. [24] through the inclusion of nitrogen in GQDs. Unlike graphene, GQDs are semiconductors with non-zero bandgap which was confirmed by previous experimental and theoretical studies. Their chemical and physical properties also vary from other carbon allotropes (graphene, CNTs, fullerene, CDs etc.) due to quantum confinement. Furthermore the investigation on GQDs is still at primeval stage and needs the light on their various matters. In order to meet the desirable application demands, further exploration for GQDs is required to enhance its properties accordingly.

### 1.3 Properties of Graphene Quantum Dots

The structural characteristics such as shape, height and edge states of GQDs count on their average size contributing fundamentally on their electronic and optical properties [25-26]. The GQDs with large size are typically polygon shaped like triangular, rectangular and hexagonal, whereas smaller size GQDs, are circular or elliptical. Fabricating GQDs through modified Hummer's method composes GQDs with diameter less than 17 nm consisting one-three graphene layers, however, for GQDs diameter greater than 22 nm, they generally consist four or more layers of graphene [25-26]. The aforementioned facts conclude that as the length of GQDs increases, the average height also increases [25-26]. The GQDs with circular and elliptical shapes exhibit both zigzag and armchair edges whereas armchair edges are found in polygonal GQDs. Moreover, crystalline nature of GQDs is identical with graphene determined through Raman spectroscopy and High-resolution transmission electron microscopy (HRTEM) [26-28]. As discussed, the electronic properties of GQDs with size 2-20 nm alters according to the edge lattice symmetry [29]. To a great extent, GQDs with size 7-8 nm and zigzag edge shows metallic nature. For GQDs with armchair edges, the energy gap ( $E_g$ ) follows  $1/L$  ranging 0-3 eV, where  $L$  is the length of edges of hexagonal GQD [30], which is in accordance with quantum confinement effect. The above relation of energy gap of GQDs contrasts other traditional quantum dots which follow the relation,  $1/L^2$ . The  $E_g$ - $L$  correlation of GQDs was fitted experimentally through power law which leads to  $E_g(eV) = 1.57 \pm 0.21 eV nm/L^{1.19 \pm 0.15}$  [29]. The  $E_g$ , excitons binding energy and spin singlet-triplet splitting are analogous to the size, edge and corner model of GQDs [31]. The overlapping of electrons and holes which is the result of spin singlet-triplet splitting decreases the possibility of non-radiative shift from the singlet to triplet state. This further leads to the high fluorescence production. These effects are the outcome of quantum confinement effect making GQDs potential candidate for optoelectronic devices like LEDs and solar cells. Approaching to the optical properties of GQDs, the broad absorption spectrum conventionally intents into intense peak in the UV range of  $\sim 4.6$ - $6.2$  eV along with tail expanding in visible range to  $\sim 2.1$  eV [21,32]. These peaks are due to  $\pi \rightarrow \pi^*$  conversion of C=C bonds and the  $n \rightarrow \pi^*$  conversion of C=O bonds, respectively [21]. The shift in absorption peak

is observed from  $\sim 6.2$  to  $\sim 4.6$  eV as the size of GQDs rises from 5 to 35 nm, due to quantum confinement effect [26] resulting near to that of graphene. The luminescent properties of GQDs are controvertible as they are originated from different parameters like shape [26], size [33], excitation wavelength [34], functional groups [35], pH [21], solvent [36] etc. For instance, the photoluminescence peak energy lowers as the GQDs size raises to  $\sim 17$  nm, which is compatible with the quantum confinement effect. Moreover, with the size enhancing above  $\sim 17$  nm, the photoluminescence (PL) peak energy increases controverting the quantum confinement effect. Thus, by controlling size and edge-state of GQDs, the electronic shifts can be improved to generate strong PL emissions [26].

#### 1.4 Synthesis Methods of Graphene Quantum Dots

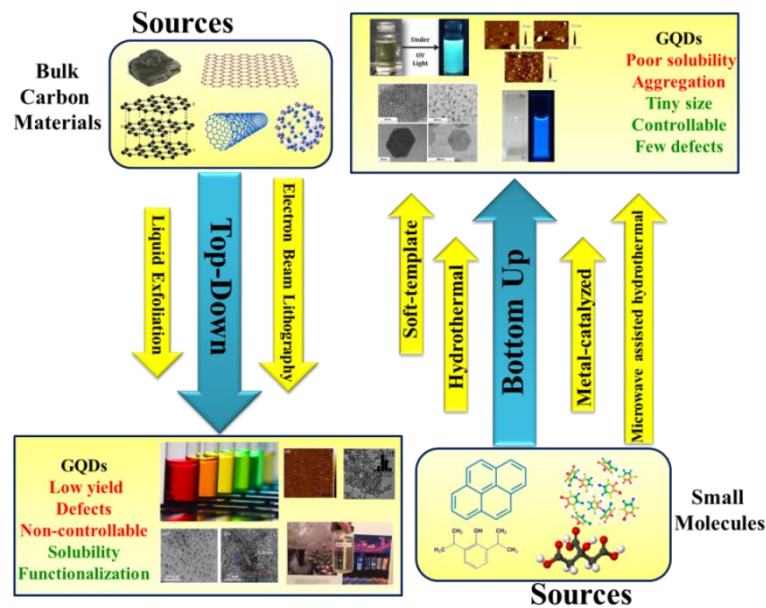


Figure 1.2: Preparation methods of graphene quantum dots.

Depending upon the GQDs fabrication methods evolving in past years, these procedures are categorically presented in two categories: (i) top-down and (ii) bottom-up (Fig. 1.2). The former method consists of direct breaking of carbon based materials (graphite, graphene, carbon nanotubes, fullerenes etc.) to nanometer-scale GQDs using techniques like liquid-phase

exfoliation, electron beam lithography approaches etc. The advantages of this method are simple, effective, plentiful raw materials yielding oxygen-containing functional groups advancing their solubility and disadvantages are low production, defects, uncontrollable size and shape. The latter method comprises growth of suitable molecular precursors like polycyclic aromatic hydrocarbon (PAHs), polymers etc. The defect, manipulate size and shape drawbacks of top-down methods were conquered in bottom-up methods. However, bottom-up method faced hurdles regarding solubility, aggregation etc. Additionally, in the area of nanomaterials the properties are evaluated through the fabrication methods. In the following perspective, comprehensive fabrication methods are demonstrated. Top-down approaches will be depicted first accompanied by bottom-up.

### 1.4.1 Top-down Methods

As discussed above, top-down method produces GQDs by cutting up the bulk materials using physical or chemical processes. This approach is efficient in the evaluation of properties of new materials discovered as the first ever graphene quantum dots were developed through top-down method. Besides other top-down methods, liquid-phase exfoliation method (via hydrothermal, oxidation, electrochemical etc.) and electron beam lithography are conventional pathways. By the use of liquid exfoliation approach, GQDs with blue luminescence was developed by Pan et al. [21]. Carbon fibers and coal were utilized as a precursor in liquid exfoliation approach to fabricate GQDs for high production yield [37-38]. Along with bulk graphite, two dimensional (2D) graphene, one dimensional (1D) carbon nanotube and zero dimensional fullerene were also be diced in GQDs [39]. However, amongst all, graphite has been considered the potential origin for the fabrication of GQDs [40-41]. The physical and chemical characteristics of GQDs can be promptly structured by altering the fabrication conditions due to the fact that liquid exfoliation method takes place in liquid and properties of precursors are evaluated using environmental conditions of the process.

Among the top-down approach, electron beam lithography was the first one to be utilized to fabricate GQDs. However, this method is not widespread due to the need of costly equipment. Regardless, electron beam lithography unlocked a significant field of 0D family of carbon materials.

### **1.4.2 Bottom-up Methods**

Bottom-up method is further categorized in four main methods, (i) hydrothermal approach, (ii) microwave-assisted hydrothermal approach, (iii) soft-template approach and (iv) metal-catalyzed.

Hydrothermal route consists of distinct ways of crystallizing materials in high-temperature liquid solutions and high vapour pressures. The PL quantum yield of 9% is acquired with ~15 nm GQDs with the help of citric acid (CA) as a precursor [42]. However, the PL quantum yield is enhanced up to 75.2% with 5-10 nm when citric acid and ethylenediamine both are used as carbon source materials in preparing nitrogen doped GQDs [43]. Besides citric acid, polyaromatic hydrocarbons (PAH) are also adapted for the fabrication of GQDs. A quick and effective microwave-assisted hydrothermal method came in the light to overcome the drawback of hydrothermal method which takes long time for the preparation of GQDs. The duration of fabrication is reduced to few minutes or seconds with the help of microwave. It was observed that using microwave-assisted hydrothermal method, GQDs with uniform size distribution were obtained [44-45]. Consequently, microwave-assisted hydrothermal route grouped the best of both worlds (hydrothermal and microwave methods). The microwave heat contributes in the uniformity of quantum dots and non-surface passivation.

For the mass production of GQDs, an economical and eco-friendly method known as soft-template method which offers nano-level reaction cavity minus any complex splitting and cleansing procedures is developed. The prominent quantum yield of 83% is evaluated by Do et al. by using citric acid as a precursor [46]. The soft-template method can be a potential approach to solve one of the concerns of GQDs fabrication like low production.

In the production of different shapes of GQDs, a new and scanty method is developed, known as the metal-catalyzed method. Fullerene as precursor with ruthenium metal catalyst is used in synthesizing triangular and hexagonal shapes of GQDs [47]. Nonetheless, this method is rare due to the presence of metal-catalyst and unique configuration of raw material.

It is noteworthy that the production yield through bottom-up method is high as compared to top-down method. Moreover, their physical and chemical properties can be altered simply in bottom-up route along with greater choices of precursors.

## 1.5 Functionalization of Graphene Quantum Dots

Pristine GQDs consists several restrictions which limit their utilization applications. In the majority of cases, functionalization is considered the best pathway to achieve the desirable performances of GQDs. Functionalization of GQDs can tune their electronic, chemical, optical properties etc. enabling them to use in various applications. Figure 1.3 presents various ways of functionalization like heteroatoms doping, development of composites with polymers or inorganic materials and regulating GQDs shape and size [48]. Functionalization is becoming the headlines to investigate carbon family in research society.

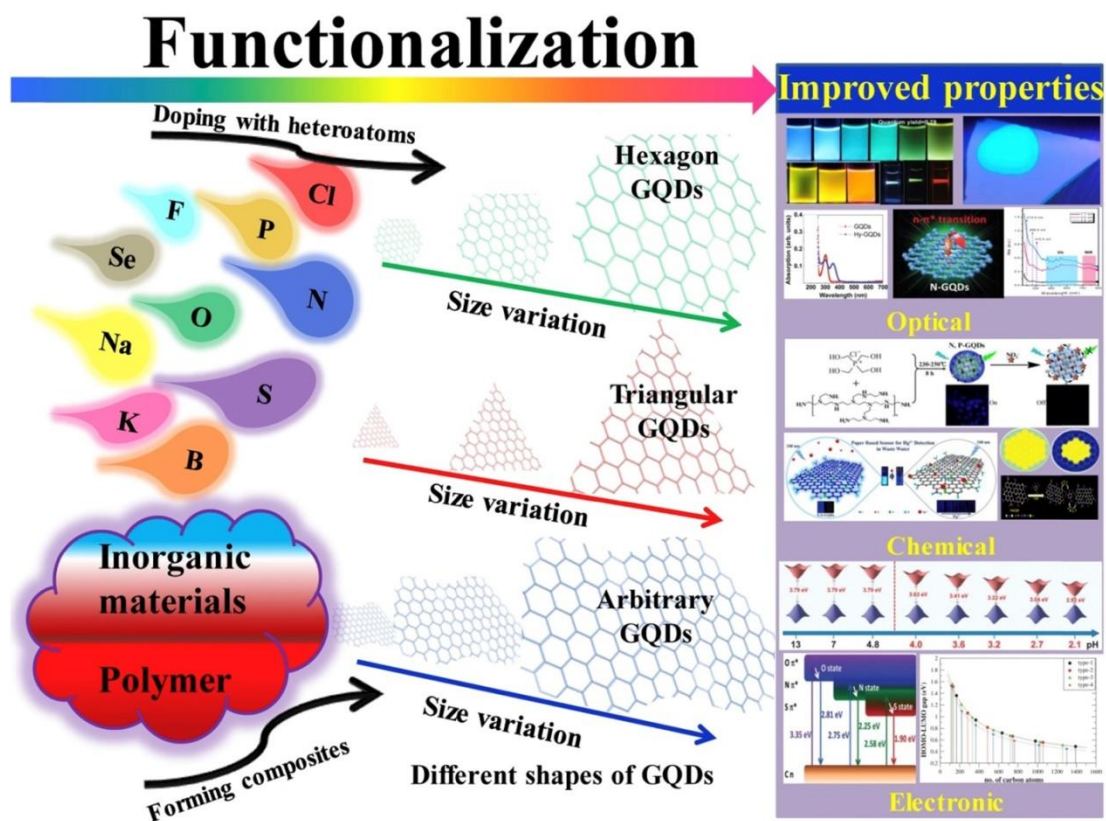


Figure 1.3: Schematic of the functionalization of GQDs through different routes and enhancement of its properties. Reproduced from Tian et al. *Mater. Today Chem.* 10, 221 (2018). Copyright 2018 Author(s), licensed under the Creative Commons License.

Doping of GQDs through variation of heteroatoms (quantity of doping atoms) can be classified in groups like (i) doping with single heteroatom, (ii) doping with two heteroatoms and (iii) doping with multiple heteroatoms. It is presented that even a single heteroatom has the capability

to modify the properties of GQDs. Boron (B) being the neighboring atom to the carbon, is easily introduced in GQDs [49-51]. The doping of B in GQDs presents improved PL and electrocatalytic activity along with the quantum yield of 95% [50-51]. Additionally, blue shift has been observed in the absorption peak of GQDs when doped with sodium (Na) [52]. It is concluded that the single heteroatom inclusion of B, K and Na in GQDs modifies their optical properties and enhances photoluminescence intensity. Among all, nitrogen atom is the first and widely studied heteroatom introduced in GQDs [43,53-55]. The phosphorus doped GQDs present better stability and scattering along with broad visible-light absorption region [56-57]. A new and unique characteristic of change in color of PL from blue to yellow has been observed in case of sulphur doping [58]. Through the doping of chlorine in GQDs multicolor light emission was attained with optical absorption peak arising in deep ultraviolet (UV) region [59-60]. After the investigation of single heteroatom doping, two atoms doping came in light for their usage [61-62]. The PL quantum yields of 61%, 45% and 8% were observed at 340, 440 and 540 nm wavelength depicting blue, green and red emission, respectively, for sulphur and nitrogen co-doped GQDs [63]. The two heteroatom doping method was certainly capable of manipulating the properties of GQDs by selecting particular doping elements for specific application. Doping of multiple heteroatoms in GQDs also play significant role in areas like batteries and solar cells. The quantum yield of 70% was acquired when GQDs is doped with fluorine (F), nitrogen (N) and sulphur (S) [64]. The addition of aforementioned dopants is also investigated for their utilization in dye-sensitized solar cells (DSSCs) with fill factor (FF) of 71% and efficiency  $11.7\% \pm 0.22$  [65].

To overcome the limitations of GQDs, functionalizing them with organic and inorganic composites is also explored for the novel applications. Organic materials have many advantages like easy formation of film, high carrier mobility, etc. to pair with the characteristics of GQDs [66-67]. Inorganic materials like ZnO [68], TiO<sub>2</sub> [69], Au nanoparticles [70], SnO<sub>2</sub> [71] with GQDs were also explored to improve the properties of GQDs for opening new areas of applications. Apart from that, the physical, chemical, electronic and optical properties of GQDs can also be altered through modulation of their shape and size. Different approaches like Raman spectroscopy [72], density of states [73], optical characterizers [74] etc. are evolved

experimentally [75] and theoretically [76-77] for size and shape dependent bandgap engineering. This technique is considered potential for the utilization of GQDs in coming times.

## 1.6 Applications of Graphene Quantum Dots



*Figure 1.4: Applications of GQDs in different fields. Reproduced from Tian et al. Mater. Today Chem. 10, 221 (2018). Copyright 2018 Author(s), licensed under the Creative Commons License.*

The properties of GQDs make them a potential candidate in diverse areas like medical, optical and energy as shown in Fig. 1.4 [78-79]. Many researches are devoted to tailor their properties in order to use them in applications like drug delivery [80], light emitting diodes (LEDs) [81], solar cells [57] etc.

### 1.6.1 Medical Applications

The GQDs have been explored recently for the medical applications attributed to their biocompatibility and non-toxicity and perhaps can substitute conventional materials. GQDs found their application in biological imaging for diagnosis by contributing in spotting cancerous cells along with finding and detecting drugs if they are delivered to the targeted cell [82]. This is due to the strong and tunable photoluminescence of GQDs. The GQDs are also considered the

worthy contestant for drug delivery due to their unique properties like carbons with  $sp^2$  bonding, abundance in  $\pi$ -electrons including carboxyl, hydroxyl, carbonyl and epoxy functional groups [83]. For the in-vivo therapeutic agent, GQDs provide superior stability, biocompatibility and therapeutic performances [84]. GQDs are also studied for antioxidants and pro-oxidants for irradiation as they consist of properties of anti-oxidants for managing reactive oxygen species (ROS) in cell harm [85]. GQDs band-aids are also designed presenting exceptional anti-bacterial property for their use in wound disinfection.

### **1.6.2 Optical Applications**

Attributed to the exceptional properties of GQDs, for instance, up-conversion, intense PL and modification of energy bandgap ( $E_g$ ) through varying size and shape various opto-devices are being presently developed [86]. Opto-electrical detectors like photodetectors, photosensors perform a significant role in national defense, space exploration etc. GQDs have gathered their attention in improving the capabilities of photodetectors due to the fact that they can be easily functionalized with unique properties. For their usage in photodetectors, GQDs composed with silicon nanowire [87], ZnO nanorods [88] and P3HT [89] have been investigated. The significant properties of GQDs lead them to be scrutinized in light emitting diodes (LEDs). Two pathways are considered for their use in LEDs, one is to cover LEDs with GQDs to amplify the strength of light and emitted wavelength [90], while second is to design LEDs structure made of GQDs [91]. An additional feature of LEDs made from GQDs is that it can alter the intensity and color of emitted light. In the carbon family, GQDs turn out to be the potential nanomaterial for photocatalysis because of their characteristics like extensive surface area, superior electron mobility, increment in lifespan of electron-hole pairs along with upconversion performance. GQDs with materials like cadmium sulfide (CdS),  $TiO_2$ , ZnO nanowires were studied leading to the enhancement in absorption intensity for visible light [92-93].

### **1.6.3 Energy-related applications**

In the period of community growth and the consumption of natural assets, it has become a necessity to research novel and renewable energy in near future. Carbon being the most abundant material can be potential material for energy applications. The important properties of GQDs like

strong luminescence, efficient functionalization, deep UV range absorption results in the advancement of using GQDs in solar cells [57,94-95]. Functionalized GQDs can improve optical absorptivity and short-circuit current leading to the high fill factor (FF) and power conversion efficiency (PCE) of 7.6% [96]. The majority of sustainable energy resources need their preservation/storage through batteries, consequently, demanding the development of capacitors with high efficacy and long-term cycling life. Lithium ion and sodium ion batteries have been broadly explored for the aforementioned purpose. However, to improve the electronic properties of batteries, GQDs can find its existence as a transporting material [97]. The presence of GQDs in batteries results in cost-effective performance and is considered essential. Another renewable and eco-friendly technology is fuel cell [98], in which functionalized GQDs gathered its attention as electrodes [99]. The improved catalytic activity and stability is due to the interior charge transfer of functionalized GQDs. Subsequently, there has been substantial growth in the investigation of GQDs as cathode material to be used in fuel cells.

### **1.7 Research Objectives**

The goal of the present thesis is to perform comprehensive first principles study based on density functional theory (DFT) of graphene quantum dots and their functionalization and further to provide the knowledge of underlying physics and chemistry behind functional group's interactions with GQDs. With improved ways in their fabrication, development and incorporation in technology, there has also been raised interest about their impact on biological, optical, electronics and environmental surrounding. Consequently, as the fabrication and utilization of GQDs remain to amplify, it is of great consequence to comprehend their effects and to develop new materials. However, the detailed objectives of the present thesis are following:

1. To obtain a better understanding of the graphene quantum dots (GQDs) structure with various size and shapes.
2. To assess the subtle differences in the electronic properties of graphene quantum dots (GQDs) with different edge structures.
3. To obtain electronic structure, electronic density of states and optical properties of GQDs and functionalized GQDs to utilize them in solar cell applications.

4. To investigate the vibrational properties of GQDs to understand the structure-dynamics-property relationship for their possible applications in surface enhanced Raman scattering (SERS).
5. To understand the binding mechanism between GQDs and functional groups to utilize them in hydrogen evolution reaction (HER) and hydrogen storage.

## **1.8 Structure of the Present Thesis**

The present thesis is systematized in the following manner. Theoretical depiction of computational methodology used throughout the work is presented in **Chapter 2**. Formalism of DFT by discussing Kohn-Sham equation to its implementation in Gaussian 09 package is discussed. Exchange-correlation along with basis sets is discussed. Time-dependent density functional theory (TD-DFT) is briefly described. Finally, applications of quantum chemical methods like geometry optimization, frequency, molecular orbitals, dipole moment and UV spectra calculations are given in present chapter.

In **Chapter 3**, the physical, electronic and magnetic properties of newly fabricated triangulene using DFT are systematically studied [100]. Triangulene, model considered for GQD, consists of two unpaired electrons due to its structure in which it is impossible to pair them. The two unpaired electrons results in triplet (ferromagnetic) and singlet (antiferromagnetic) orientations. Present study depicts that triplet (ferromagnetic) state is more stable as compared to its singlet (antiferromagnetic) state. The findings of the study shows that the characteristics of GQDs can be utilized in spin electronics and magnetic carbon materials. Additionally, the effect of magnetic elements iron (Fe), cobalt (Co), nickel (Ni) and copper (Cu) on triangulene is also investigated for their possible usage in the spin electronics. The study suggests that doping magnetic elements in GQDs can be used to store information in information readout devices.

**Chapter 4** consists of study related to hydrogen evolution reaction (HER) activity on triangulene using first principles based DFT through adsorption mechanism and electronic structure calculations [101]. Triangulene presents better HER activity with adsorption energy ( $E_{ad}$ ) of -0.264, when hydrogen is placed over top site of carbon, which is in the vicinity of Gibbs free energy. The free energy calculation of triangulene for HER depicts that it is suitable catalyst

among all quantum dots. Further, for the exploration of GQDs to be utilized in hydrogen storage, triangulene with platinum at different sites is investigated. The study shows that platinum atom considers hollow site as compared to other top and bridge sites. The density of states (DOS), highest orbital molecular orbital (HOMO), lowest unoccupied molecular orbitals (LUMO) and HOMO-LUMO gap ( $E_g$ ) is demonstrated for the validation of hydrogen storage over platinum decorated triangulene. The results conclude that hydrogen ( $H_2$ ) is dissociated over all hollow, top and bridge sites leading to the D-mode. This underlying insight of adsorption mechanism including study of electronic properties will be essential for spillover mechanism and design of efficient GQDs for hydrogen storage applications.

In **Chapter 5**, the influence of heteroatoms nitrogen (N), boron (B) and phosphorus (P) is explored on carboxyl group edge-functionalized graphene quantum dots (COOH-GQDs) for their possible application in novel, non-toxic and efficient quantum dot-sensitized solar cells (QDSCs) [57]. The HOMO, LUMO,  $E_g$  along with binding process, electrostatic potential, and Mulliken charge transfer are studied to examine the modification in electron inclusion and charge splitting in pristine and doped COOH-GQDs. The calculation of optical properties presents wide spectrum in visible range to yield solar light. To foresee the utilization of N/B/P doped COOH-GQD in QDSCs, the solar cell parameters like open circuit voltage ( $V_{oc}$ ), fill factor (FF), short circuit current density ( $J_{sc}$ ) and power conversion efficiency ( $\eta$ ) are evaluated. After the doping of adatoms in COOH-GQDs, the efficiency is enhanced up to 22-30%. The maximum efficiency is attained in P doped COOH-GQD attributed to its electron donating nature resulting in additional electron inclusion to the  $TiO_2$  surface. The results depict that these new sensitizers predicted on GQDs can be potential candidates for future QDSCs applications.

With the aim to monitor melamine due to its harmful effects on human, (i) oxygen (O) and sulphur (S) doped COOH-GQDs (ii) pristine and functionalized rectangular GQDs with three different sites (hollow, bridge and top sites), have been used and presented in **Chapter 6** [102,103]. An efficient vibrational spectroscopic method, surface enhanced Raman scattering (SERS) is chosen to detect and filter melamine. The structural, electronic and vibrational properties are studied by means of DFT. In case of O-GQD and S-GQD, adsorption energy is calculated to check the binding mechanism which is -1.18 eV and -0.15 eV respectively. It is

found that the intense peak at  $688\text{ cm}^{-1}$  increases by 348.4% and 48% for Mel-O-GQD and Mel-S-GQD. The chemical enhancement factor (*EF*) is also evaluated with the values of 4.51 and 1.48 for Mel-O-GQD and Mel-S-GQD respectively, which is ever higher than melamine adsorbed over silver complexes. In the next study of present chapter, the adsorption energy is -0.16 eV in pristine GQD which increases to -0.53 eV in *f*-GQD. The high EF of 39.89 is found for peak  $736\text{ cm}^{-1}$ . The work concludes that doped as well as functionalized GQDs could be promising platforms for the sensing of melamine.

The results of systematic investigation on structural, electronic, vibrational and magnetic properties of various size and shape GQDs along with their functionalization have been summarized in **Chapter 7**. Variation of properties of functionalization compared to their pristine counterpart has been concluded discussing promising applications of GQDs in science and technology followed by a brief discussion on potential future works.

## Reference

1. B. C. Brodie, *Phil. Trans. Roy. Soc. Lond.* **149** (1859) 249-259.
2. V. Kohlschütter, P. Haenni, *Z. Anorg. Allg. Chem.* **105** (1919) 121-144.
3. J. D. Bernal, *Proc. R. Soc. Lond. Ser. A Contain. Pap. Math. Phys. Character* **106** (1924) 749-773.
4. P. R. Wallace, *Phys. Rev.* **71** (1947) 622-634.
5. G. Ruess, F. Vogt, *Monatsh. Chem.* **78** (1948) 222-242.
6. W. S. Hummers, R. E. Offeman, *J. Am. Chem. Soc.* **80** (1958) 1339-1339.
7. H. P. Boehm, A. Clauss, G.O. Fischer, U. Hofmann, *Z. Anorg. Allg. Chem.* **316** (1962) 119-127.
8. D. DiVincenzo, E. Mele, *Phys. Rev. B* **29** (1984) 1685-1694.
9. H.W. Kroto, J.R. Heath, S.C. O'Brien, R.F. Curl, R.E. Smalley, *Nature* **318** (1985) 162-163.
10. S. Mouras, A. Hamwi, D. Djurado, J.-C. Cousseins, *Rev. Chim. Miner.* **24** (1987) 572-582.
11. S. Iijima, *Nature* **354** (1991) 56-58.

12. K. S. Novoselov, A. K. Geim, S. V. Morozov, D. Jiang, Y. Zhang, S. V. Dubonos, I. V. Grigorieva, A. A. Firsov, *Science* **306** (2004) 666-669.
13. A. H. Castro Neto, F. Guinea, N. M. R. Peres, K. S. Novoselov, A. K. Geim, *Rev. Mod. Phys.* **81** (2009) 109-162
14. C. Lee, X. Wei, J. W. Kysar, J. Hone, *Science* **321** (2008) 385–388.
15. R. R. Nair, P. Blake, A. N. Grigorenko, K. S. Novoselov, T. J. Booth, T. Stauber, N. M. R. Peres, A. K. Geim, *Science* **320** (2008) 1308–1308.
16. S. Ren, P. Rong, Q. Yu, *Ceramics International* **44** (2018) 11940-11955.
17. I. Meric, M. Y. Han, A. F. Young, *Nat. Nanotechnol.* **3** (2008) 654–659.
18. X. Y. Xu, R. Ray, Y. L. Gu, H. J. Ploehn, L. Gearheart, K. Raker, W. A. Scrivens, *J. Am. Chem. Soc.* **126** (2004) 12736-12737.
19. L. A. Ponomarenko, F. Schedin, M. I. Katsnelson, R. Yang, E. W. Hill, K. S. Novoselov, A. K. Geim, *Science* **320** (2008) 356-358.
20. D. Wang, J.-F. Chen, L. Dai, *Part. Part. Syst. Char* **5** (2015) 515-523.
21. D. Pan, J. Zhang, Z. Li, M. Wu, *Adv. Mater.* **6** (2010) 734-738.
22. Y. Jang, A. Shapiro, M. Isarov, A. Rubin-Brusilovski, A. Safran, A. K. Budniak, F. Horani, J. Dehnel, A. Sashchiuk, E. Lifshitz, *Chem. Commun.* **53** (2017) 1002-1024.
23. P. Reiss, M. Protière, L. Li, *Small* **5** (2009), 154-168.
24. Y. Zhao, C. G. Hu, Y. Hu, H. H. Cheng, G. Q. Shi, L. T. Qu, *Angew. Chem. Int. Ed.* **51** (2012) 11371-11375.
25. D. B. Shinde, V. K. Pillai, *Chem. Eur. J.* **18** (2012) 12522–12528.
26. S. Kim et al., *ACS Nano* **6** (2012) 8203–8208.
27. S. Zhu, S. Tang, J. Zhang, B. Yang, *Chem. Commun.* **48** (2012) 4527–4539
28. S. Kim, D. H. Shin, C. O. Kim, S. S. Kang, S. S. Joo, S. H. Choi, S. W. Hwang, C. Sone, *Appl. Phys. Lett.* **102** (2013) 053108.
29. K. A. Ritter, J. W. Lyding, *Nat. Mater.* **8** (2009) 235–242.
30. Z. Z. Zhang, K. Chang, F. M. Peeters, *Phys. Rev. B* **77** (2008) 235411.
31. Y. Li, H. Shu, S. Wang, J. Wang, *J. Phys. Chem. C* **119** (2015) 4983–4989.

- 
32. L. Yang, J. Deslippe, C. H. Park, M. L. Cohen, S. G. Louie, *Phys. Rev. Lett.* **103** (2009) 186802
  33. W. Kwon, Y. H. Kim, C. L. Lee, M. Lee, H. C. Choi, T. W. Lee, S. W. Rhee, *Nano Lett.* **14** (2014) 1306–1311.
  34. C. Hu, Y. Liu, Y. Yang, J. Cui, Z. Huang, Y. Wang, L. Yang, H. Wang, Y. Xiao, J. Rong, *J. Mater. Chem. B* **1** (2013) 39–42.
  35. F. Liu, M. H. Jang, H. D. Ha, J. H. Kim, Y. H. Cho, T. S. Seo, *Adv. Mater.* **25** (2013) 3657–3662
  36. D. Pan, C. Xi, Z. Li, L. Wang, Z. Chen, B. Lu, M. Wu, *J. Mater. Chem. A* **1** (2013) 3551–3555
  37. J. Peng, W. Gao, B. K. Gupta, Z. Liu, R. Romero-Aburto, L. Ge, L. Song, L. B. Alemany, X. Zhan, G. Gao, S. A. Vithayathil, B. A. Kaiparettu, A. A. Marti, T. Hayashi, J.-J. Zhu, P. M. Ajayan, *Nano Lett.* **2** (2012) 844-849.
  38. R. Ye, C. Xiang, J. Lin, Z. Peng, K. Huang, Z. Yan et al., *Nat. Commun.* **4** (2013) 2943.
  39. Y. Dong, H. Pang, S. Ren, C. Chen, Y. Chi, T. Yu, *Carbon* **64** (2013) 245-251.
  40. S. Sarkar, D. Gandla, Y. Venkatesh, P. R. Bangal, S. Ghosh, Y. Yang, S. Misra, *Phys. Chem. Chem. Phys.* **18** (2016) 21278-21287.
  41. M. Xu, W. Zhang, Z. Yang, F. Yu, Y. Ma, N. Hu, D. He, Q. Liang, Y. Su, Y. Zhang, *Nanoscale* **7** (2015) 10527-10534.
  42. Y. Dong, J. Shao, C. Chen, H. Li, R. Wang, Y. Chi, X. Lin, G. Chen, *Carbon* **12** (2012) 4738-4743.
  43. J. Gu, X. Zhang, A. Pang, J. Yang, *Nanotechnology* **27** (2016) 165704.
  44. L. Tang, R. Ji, X. Li, K. S. Teng, S. P. Lau, *Part. Part. Syst. Char.* **6** (2013) 523-531.
  45. L. Tang, R. Ji, X. Cao, J. Lin, H. Jiang, X. Li, K. S. Teng, C. M. Luk, S. Zeng, J. Hao, S. P. Lau, *ACS Nano* **6** (2012) 5102-5110.
  46. S. Do, W. K. S.-W. Rhee, *J. Mater. Chem. C* **2** (2014) 4221-4226.
  47. J. Lu, P. S. E. Yeo, C. K. Gan, P. Wu, K. P. Loh, *Nat. Nanotechnol.* **4** (2011) 247-252.
  48. P. Tian, L. Tang, K. S. Teng, S. P. Lau, *Mater. Today Chem.* **10** (2018) 221-258.

49. X. Hai, Q.-X. Mao, W.-J. Wang, X.-F. Wang, X.-W. Chen, J.-H. Wang, *J. Mater. Chem. B* **3** (2015) 9109-9114.
50. Z. Fan, Y. Li, X. Li, L. Fan, S. Zhou, D. Fang, S. Yang, *Carbon* **70** (2014) 149-156.
51. T. V. Tam, S. G. Kang, K. F. Babu, E.-S. Oh, S.G. Lee, W.M. Choi, *J. Mater. Chem. A* **5** (2017) 10537-10543.
52. N.-U. Ain, M. O. Eriksson, S. Schmidt, M. Asghar, P.-C. Lin, P. O. Holtz, M. Syväjärvi, G.R. Yazdi, *Nanomaterials* **6** (2016) 198.
53. Y. Zhao, C. G. Hu, Y. Hu, H. H. Cheng, G. Q. Shi, L. T. Qu, *Angew. Chem. Int. Ed.* **51** (2012) 11371-11375.
54. L. Lin, M. Rong, S. Lu, X. Song, Y. Zhong, J. Yan, Y. Wang, X. Chen, *Nanoscale* **7** (2015) 1872-1878.
55. S. Gao, L. Tang, J. Xiang, R. Ji, S. K. Lai, S. Yuan, S.P. Lau, *New J. Chem.* **18** (2017) 10447-10451.
56. J. Qian, C. Shen, J. Yan, F. Xi, X. Dong, J. Liu, *J. Phys. Chem. C* **122** (2018) 349-358.
57. V. Sharma, P. K Jha, *Sol. Energy Mater. Sol. Cells* **200** (2019) 109908.
58. G. Wang, G. Guo, D. Chen, Z. Liu, X. Zheng, A. Xu, S. Yang, G. Ding, *ACS Appl. Mater. Interfaces* **10** (2018) 5750-5759.
59. X. Li, S.P. Lau, L. Tang, R. Ji, P. Yang, *J. Mater. Chem. C* **1** (2013) 7308-7313.
60. J. Zhao, L. Tang, J. Xiang, R. Ji, J. Yuan, J. Zhao, R. Yu, Y. Tai, L. Song, *Appl. Phys. Lett.* **105** (2014) 111116.
61. R. S. Li, B. Yuan, J. H. Liu, M. L. Liu, P. F. Gao, Y. F. Li, M. Li, C. Z. Huan, *J. Mater. Chem. B* **5** (2017) 8719-8724.
62. T. K. Mondal, D. Dinda, S. K. Saha, *Sensor. Actuator. B* **207** (2018) 586-593.
63. D. Qu, Z. Sun, M. Zheng, J. Li, Y. Zhang, G. Zhang, H. Zhao, X. Liu, Z. Xie, *Adv. Opt. Mater.* **3** (2015) 360-367.
64. S. Kundu, R. M. Yadav, T. N. Narayanan, M. V. Shelke, R. Vajtai, P. M. Ajayan, V. K. Pillai, *Nanoscale* **7** (2015) 11515-11519.

- 
65. S. Kundu, P. Sarojinijeeva, R. Karthick, G. Anantharaj, G. Saritha, R. Bera, S. Anandan, A. Patra, P. Ragupathy, M. Selvaraj, D. Jeyakumar, K.V. Pillai, *Electrochim. Acta* **242** (2017) 337-343.
66. T. Wen, B. Yang, Y. Guo, J. Sun, C. Zhao, S. Zhang, M. Zhang, Y. Wang, *Phys. Chem. Chem. Phys.* **16** (2014) 23188-23195.
67. Q. Chen, Y. Hu, C. Hu, H. Cheng, Z. Zhang, H. Shao, L. Qu, *Phys. Chem. Chem. Phys.* **16** (2014) 19307-19313.
68. S. Dhar, T. Majumder, S. P. Mondal, *Mater. Res. Bull.* **95** (2017) 198-203.
69. X. Bu, S. Yang, Y. Bu, P. He, Y. Yang, G. Wang, H. Li, P. Wang, X. Wang, G. Ding, J. Yang, X. Xie, *ChemistrySelect* **3** (2018) 12260-12265.
70. X. Wu, S. Guo, J. Zhang, *Chem. Commun.* **51** (2015) 6318-6321.
71. X. Chu, J. Wang, J. Zhang, Y. Dong, W. Sun, W. Zhang, L. Bai, *J. Mater. Sci.* **52** (2017) 9441-9451.
72. S. Kim, D. H. Shin, C. O. Kim, S. S. Kang, S. S. Joo, S.-H. Choi, S.W. Hwang, C. Sone, *Appl. Phys. Lett.* **102** (2013) 053108.
73. T. Espiosa-Ortega, I. A. Luk'Yanchuk, Y. G. Rubo, *Superlattice Microst.* **49** (2011) 283-287.
74. R. Zhang, S. Qi, J. Jia, B. Torre, H. Zeng, H. Wu, X. Xu, *J. Alloy. Comp.* **623** (2015) 186-191.
75. H. Yang, K.H. Ku, J.M. Shin, J. Lee, C.H. Park, H.-H. Cho, S.G. Jang, B.J. Kim, *Chem. Mater.* **28** (2016) 830-837.
76. P. Zhang, Q. Hu, X. Yang, X. Hou, J. Mi, L. Liu, M. Dong, *RSC Adv.* **8** (2018) 531-536.
77. P. Elvati, E. Baumeister, A. Violi, *RSC Adv.* **7** (2017) 17704-17710.
78. P. Sudhagar, I. Herraiz-Cardona, H. Park, T. Song, S. H. Noh, S. Gimenez, I. M. Sero, F. Fabregat-Santiago, J. Bisquert, C. Terashima, U. Paik, Y. S. Kang, A. Fujishima, T. H. Han, *Electrochim. Acta* **187** (2016) 249-255.
79. H. Liu, W. Na, Z. Liu, X. Chen, X. Su, *Biosens. Bioelectron.* **92** (2017) 229-233.
80. D. Wu, Y. Liu, Y. Wang, L. Hu, H. Ma, G. Wang, Q. Wei, *Sci. Rep.* **6** (2016) 20511.

- 
81. C. Xu, S. Yang, L. Tian, T. Guo, G. Ding, J. Zhao, J. Sun, J. Lu, Z. Wang, *Appl. Phys. Express* **10** (2017) 032102.
  82. K.L. Schroeder, R.V. Goreham, T. Nann, *Pharm. Res.* **33** (2016) 2337-2357.
  83. Y.-L. Su, T.-W. Yu, W.-H. Chiang, H.-C. Chiu, C.-H. Chang, C.-S. Chiang, S.-H. Hu, *Adv. Funct. Mater.* **27** (2017) 1700056.
  84. H. Dong, W. Dai, H. Ju, H. Lu, S. Wang, L. Xu, S.F. Zhou, Y. Zhang, X. Zhang, *ACS Appl. Mater. Interfaces* **7** (2015) 11015-11023.
  85. M. J. Birnkrant, K. Bell, S. Coreth, P. R. Harris, A. M. Vincitore, J. M. Alexander, *ACS Nano* **10** (2016) 8690-8699.
  86. X. Qin, X. Liu, W. Huang, M. Bettinelli, X. Liu, *Chem. Rev.* **117** (2017) 4488-4527.
  87. I. Mihalache, A. Radoi, R. Pascu, C. Romanitan, E. Vasile, M. Kusko, *ACS Appl. Mater. Interfaces* **9** (2017) 29234-29247.
  88. M.-L. Tsai, D.-S. Tsai, L. Tang, L.-J. Chen, S.P. Lau, J.-H. He, *ACS Nano* **11** (2017) 4564-4570.
  89. J. Zhao, L. Tang, J. Xiang, R. Ji, Y. Hu, J. Yuan, J. Zhao, Y. Tai, Y. Cai, *RSC Adv.* **5** (2015) 29222-29229.
  90. J. Zhu, X. Bai, X. Chen, Z. Xie, Y. Zhu, G. Pan, Y. Zhai, H. Zhang, B. Dong, H. Song, *Dalton Trans.* **47** (2018) 3811-3818.
  91. R. Sekiya, Y. Uemura, H. Murakami, T. Haino, *Angew. Chem. Int. Ed.* **53** (2014) 5619-5623.
  92. Y. Lei, C. Yang, J. Hou, F. Wang, S. Min, X. Ma, Z. Jin, J. Xu, G. Lu, K.-W. Huang, *Appl. Catal. B Environ.* **216** (2017) 59-69.
  93. J. Tang, Y. Liu, Y. Hu, G. Lv, C. Yang, G. Yang, *Chem. Eur J.* **24** (2018) 4390-4398.
  94. S. Diao, X. Zhang, Z. Shao, K. Ding, J. Jie, X. Zhang, *Nano Energy* **31** (2017) 359-366.
  95. A. Kolay, R.K. Kokal, A. Kalluri, I. Macwan, P. K. Patra, P. Ghosal, M. Deepa, *ACS Appl. Mater. Interfaces* **9** (2017) 34915-34926.
  96. J. K. Kim, M. J. Park, S. J. Kim, D. H. Wang, S. P. Cho, S. Bae, J. H. Park, B. H. Hong, *ACS Nano* **7** (2013) 7207-7212.

97. D. Chao, C. Zhu, X. Xia, J. Liu, X. Zhang, J. Wang, P. Liang, J. Lin, H. Zhang, Z.X. Shen, H. J. Fan, *Nano Lett.* **15** (2015) 565-573.
98. S. Bose, T. Kuila, T. X. H. Nguyen, N. H. Kim, K-T. Lau, J.H. Lee, *Prog. Polym. Sci.* **36** (2011) 813-843.
99. H. Fei, R. Ye, G. Ye, Y. Gong, Z. Peng, X. Fan, E.L.G. Samuel, P.M. Ajayan, J.M. Tour, *ACS Nano* **8** (2014) 10837-10843.
100. V. Sharma, N. Som, S. D. Dabhi, P. K. Jha, *ChemistrySelect* **3** (2018) 2390-2397.
101. V. Sharma, H. L. Kagdada, Jinlan Wang, P. K. Jha, *Int. J. Hydrog. Energy*. Doi: 10.1016/j.ijhydene.2019.09.021
102. V. Sharma, N. N. Som, S. B. Pillai, P. K. Jha, *Spectrochim. Acta A* **224** (2020) 117352.
103. V. Sharma, H. L. Kagdada, D. K. Singh, P. K. Jha, *In: Singh D., Das S., Materny A. (eds) Advances in Spectroscopy: Molecules to Materials. Springer Proceedings in Physics, vol 236. Springer, Singapore* (2019).